2024 SICASH
SLIIT INTERNATIONAL CONFERENCE ON ADVANCEMENTS IN SCIENCES & HUMANITIES

A Study on *Conscinium fenestratum* and Chitosan Biopolymer Composite for Ayurvedic Drug Delivery

Manisha Alwis[1], Madara Jayanetti[2], Charitha Thambiliyagodage*[3]
[1,2,3]*Sri Lanka Institute of Information Technology*
Email address of the corresponding author -*charitha.t@sliit.lk

Abstract

This study delves into the synergistic amalgamation of *Coscinium fenestratum*, an Ayurvedic medicinal plant, and chitosan biopolymer. This results in the innovative Venivel Chitosan Composite, which has established a pioneering drug delivery system. Subsequently, the composite material, Venivel Chitosan Composite, was formulated by integrating *Coscinium fenestratum* extract and chitosan biopolymer. Structural characteristics of Chitosan biopolymer and Venivel Chitosan Composite were determined via scanning electron microscopy (SEM), offering valuable insights into their morphological features. Furthermore, a comprehensive characterization of the composite was achieved through the analysis of X-ray diffraction (XRD) patterns, elucidating its crystalline structure. A meticulous examination of the in vitro drug release profile revealed a predominant diffusion mechanism, indicating the potential suitability of this system for applications in wound healing treatments. In conclusion, integrating *Coscinium fenestratum* with chitosan biopolymer presents a versatile composite with promising antibacterial, antioxidant, and anti-inflammatory properties, elevating its potential for targeted and controlled ayurvedic drug delivery applications.

Keywords: *Coscinium fenestratum;* Drug delivery; Chitosan

Introduction

Coscinium fenestratum, a critically endangered medicinal plant from the Menispermaceae family, grows in India's moist deciduous to evergreen forests and Sri Lanka's Western Ghats at 350-1200m altitudes. The plant is known for its diverse medicinal properties and is used in traditional medicine to treat diabetes mellitus, microbial infections, and other ailments. The plant stem has anti-microbial, anti-diabetic, anti-inflammatory, and antioxidant properties, while the root is used for wound dressing, ulcer treatment, and as an antibacterial agent. The stem extract is effective against snake bites, and the bark is used to treat fevers, malarial fever in Sri Lanka, and herpes in coastal Karnataka, India. Berberine is the principal constituent of *Coscinium fenestratum*, known for its yellow crystalline alkaloid form. Other compounds in the stem include ceryl alcohol, hentriacontane, sitosterol, palmitic acid, oleic acid, and saponin. The root contains tertiary alkaloids like berlambine, dihydroberlambine, and noroxyhydrastinine. Protoberberine alkaloids, quaternary alkaloids, and minor alkaloids like palmatine and jatrorrhizine are also present. The stem of *Coscinium fenestratum* exhibits various medicinal uses, including anti-acne, anti-inflammatory, antioxidant, hypotensive, antiplasmodial, antibacterial, antidiabetic, antiproliferative, antihepato toxic,

https://doi.org/10.54389/WPRL5677

CNS depressant, and analgesic properties. Berberine shows pharmacological effects against hypertension, cancers, bacteria, inflammation, and HIV. The plant's antibacterial activity is primarily attributed to berberine. The methanolic extract of *Coscinium fenestratum* increases antioxidant enzyme activity, combating oxidative stress caused by liver damage. Its high scavenging property is due to hydroxyl groups in phenolic compounds, aiding in natural cancer defense mechanisms. The antibacterial activity of the plant is due to berberine, with extracts showing inhibitory effects on Clostridium tetani, Propionibacterium acnes, and Staphylococcus epidermidis.

Chitin, the second most abundant biopolymer after cellulose, comprises N-acetylglucosamine monomers linked by β-1,4 glycosidic bonds. Chitosan, derived from chitin, is a polycationic heteropolysaccharide with biological properties such as antioxidant, anti-inflammatory, and antimicrobial activities. Chitosan is widely used in tissue engineering, drug delivery, and other biomedical applications due to its biocompatibility and biodegradability. Chitosan's unique properties make it ideal for drug delivery applications. Classified as "Generally Recognized as Safe" (GRAS) by the FDA, chitosan is used in various delivery systems for targeted and prolonged drug release, extending to bone regeneration, wound healing, and gene transfer. Copper oxide nanoparticles exhibit significant antimicrobial and biocide properties. Their optical, electrical, and magnetic properties vary based on synthesis methods like the sonochemical and sol-gel methods. The size, morphology, and crystallinity of CuO NPs are crucial for their application in various fields, including cosmetics, pharmacology, and coatings.

Drug release systems deliver drugs efficiently and accurately through immediate, extended, and triggered release mechanisms. Mathematical models help understand and predict drug release behavior, essential for tuning therapeutic parameters. The Korsmeyer-Peppas model describes the exponential relationship between drug release and time, the Peppas-Sahlin model considers diffusion and macromolecule relaxation, and the Higuchi model describes drug release through diffusion. The Zero Order Model represents a linear drug release profile independent of concentration, while the First Order Model correlates with the drug amount in the matrix. The Hixson-Crowell Model assumes drug release is limited by dissolution rate and matrix erosion.

Methodology

1.1. Chemicals and Materials

Coscinium fenestratum stems were sourced from Sri Lanka in June 2023. Methanol and Isopropyl Alcohol were purchased from Athula Laboratory Equipment. Shrimp shells (*Penaeus vannamei*) were obtained from Ceylon Catch (Pvt) Ltd. HCl, HNO_3, and NaOH pellets from Sigma Aldrich and Sisco Research Laboratories. All chemicals were analytical grade.

1.2 Preparation of the plant extract

Dried stems of *Coscinium fenestratum* were chopped, washed, and dried at 40 °C. The stems were ground into a fine powder and stored in an airtight container. *Coscinium fenestratum* powder (10 g) was mixed with 50 mL of 80% methanol and sonicated for 3 hours at 40 °C. The supernatant was collected after centrifugation, and a double extraction was performed. The methanolic extract was stored in an airtight container.

1.3 Synthesis of Chitosan from Shrimp Shells

Shrimp shells were washed, dried, and ground into a fine powder. The powder was demineralized using 10% HCl and deproteinization with 3% NaOH. Deacetylation was achieved by refluxing in 50% NaOH, yielding chitosan, which was then dried and stored.

1.4 Preparation of *Coscinium fenestratum* and Chitosan Composite

The methanolic extract was evaporated to 25 mL and mixed with 1g of chitosan at 40°C. The composite was stirred overnight, dried, and stored as a fine powder.

1.5 Determining the antimicrobial, anti-inflammatory and antioxidant properties of *Coscinium fenestratum* and Chitosan Composite

The antimicrobial, anti-inflammatory and antioxidant properties of *Coscinium fenestratum* and Chitosan Composite was determined through agar well diffusion method, egg albumin denaturation assay and DPPH free radical scavenging method.

Results and Discussion

2.1 XRD Analysis

X-ray diffraction patterns were gathered to understand the crystal nature of the synthesized composites. The XRD pattern of Chitosan is depicted in Figure 35. The XRD pattern showed a broad peak at 19.47°. XRD patterns of Chitosan showed peaks at 2θ, 12.9, 19.47, 20.91,23.18, 26.48, 28.7, 34.84, 39.13 and 48.25°. The XRD pattern of the Venivel Chitosan Composite is depicted in Figure 34. The XRD pattern showed broad peaks at 19.34, 35.5 and 38.76°. XRD patterns of VCC showed peaks at 2θ, 19.34, 23.48, 32.38, 35.5, 38.76, 48.76, 53.68, 58.46, 61.42, 66.22, 68.12, 72.3 and 75.08°.

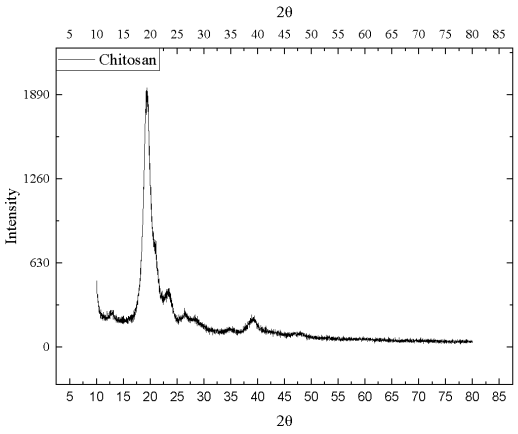

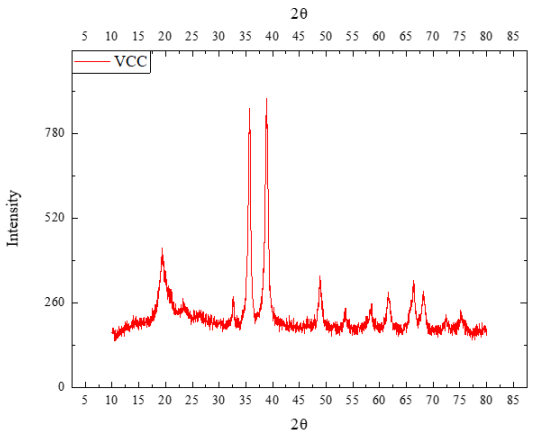

Figure 1. The XRD patterns of (a) chitosan (b) Venivel/ chitosan composite

The interlayer distance and crystallite size were calculated using the equations below.

Where λ—wavelength of the X-ray source; θ—diffraction angle; L—crystallite size; β—half maximum of the peak in radians; K—Scherer's constant (0.9). Chitosan showed an interlayer distance of 4.244 nm with a crystallite size of 0.6481 nm, whereas the composite showed an interlayer distance of 2.321 nm and a crystallite size of 13.44 nm.

3.2 SEM Analysis

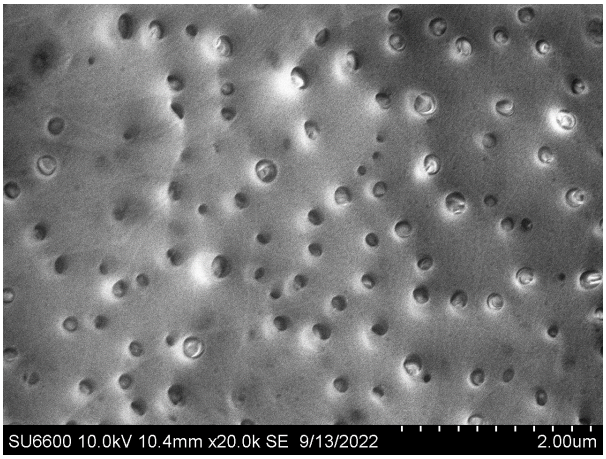

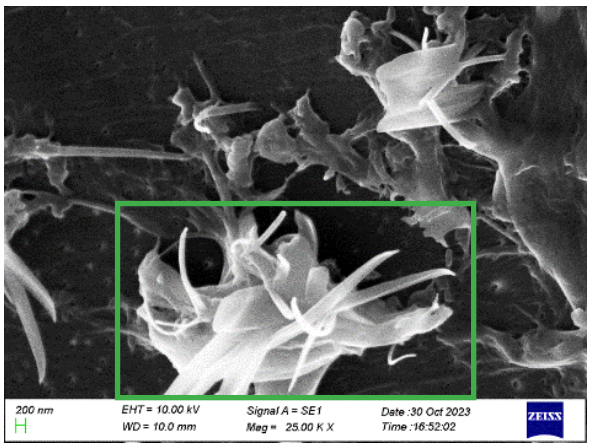

Figure 2. SEM images of (a) chitosan (b) venivel-chitosan composite

The SEM image of Chitosan reveals a surface structure with macropores on the surface. The image also depicts the presence of a slight fibrous structure. SEM images of Venivel Chitosan Composite showed a thread-like structure.

3.3 In vitro release of Venivel Chitosan Composite and kinetic study

The release behavior of VCC was evaluated by suspending the composite in a series of pH solutions and NaCl solutions and was measured by a UV-Vis spectrometer. According to a study conducted by (Asadian-Ardakani et al., 2016a), the cumulative drug release was calculated using the following equation:

$$\text{Cumulative drug release} \quad (\%) = \frac{\text{CrVr}}{\text{CoVo-CtVt}} \text{ X } 100$$

Cr and Vr are the solution's concentration and volume after the drug's release. In addition, C_0V_0-C_tV_t is the weight of the loaded drug in the system (Asadian-Ardakani et al., 2016b).

The mathematical modeling of drug release kinetics was employed to observe and analyze the mass transport mechanisms responsible for controlling drug release. (Asadian-Ardakani et al., 2016a). The mechanism of drug release was investigated using six kinetic models: Korsmeyer–Peppas, Peppas – Sahlin, Higuchi model, Zero Order, First Order, and Hixson–Crowell model, and calculated parameters varying the pH, ionic strength, and different weights of the drug are tabulated in table 1, 2 and 3, respectively.

Table 1. Parameters of Korsmeyer–Peppas, Peppas – Sahlin, Higuchi model, Zero Order, First Order, and Hixson–Crowell model of VCC drug release in pH solutions.

Model / Parameters	pH 1	pH 2.5	pH 4	pH 5.5	pH 7	pH 7.4	pH 8.5	pH 10
Korsmeyer–Peppas								
K	39.581314	35.11567	34.651	19.79	37.7724	39.24	18.92	27.91
N	0.0129498	0.017224	0.023	0.038	0.01263	0.012	0.064	0.048
R^2	0.9743094	0.988714	0.9909	0.974	0.9694	0.988	0.993	0.974
Peppas - Sahlin								
Kd	0	27.79243	27.052	14.79	29.0125	17.5	14.63	0
Kr	39.581225	7.326703	7.6054	5.003	8.76122	21.74	4.327	27.91
M	0.0064753	0.014165	0.0187	0.03	0.01021	0.007	0.05	0.024
R^2	0.9743093	0.988744	0.9909	0.975	0.96959	0.988	0.993	0.974
Higuchi model								
Kh	3.3811594	3.064702	3.1114	1.921	3.22314	3.522	2.078	2.834
R^2	0.8633742	0.917562	0.9182	0.971	0.93868	0.865	0.933	0.949
Zero Order								
K0	0.2285651	0.207395	0.2107	0.131	0.218007	0.252	0.142	0.02
R^2	0.7297606	0.805164	0.8045	0.901	0.83904	0.735	0.828	0.854

First Order								
K1	0.5233279	0.474572	0.4823	0.298	0.044143	0.577	0.323	0.441
R^2	0.7297606	0.805164	0.8045	0.901	0.83904	0.735	0.828	0.854
Hixson–Crowell model								
Khc	0.1444254	0.142058	0.13359	0.083	0.138322	0.154	0.023	0.123
R^2	0.738928	0.8199032	0.816	0.91	0.844673	0.743	0.979	0.871

Table 2. Parameters of Korsmeyer–Peppas, Peppas – Sahlin, Higuchi model, Zero Order, First Order, and Hixson–Crowell model of VCC drug release in NaCl solutions.

Model / Parameters	0.1 M NaCl	0.2 M NaCl	0.3 M NaCl	0.4 M NaCl	0.5 M NaCl
Korsmeyer–Peppas					
K	33.9384881	34.0301709	30.742002	31.0107946	26.2623005
N	0.02431205	0.0303515	0.0165293	0.02428237	0.04469735
R^2	0.98026689	0.97213951	0.98755471	0.96061366	0.99051288
Peppas - Sahlin					
Kd	26.7610999	26.1005276	26.5299714	26.7439836	22.6463449
Kr	7.18886596	7.94244558	4.21377446	4.26833738	3.63287824
M	0.01986711	0.02432876	0.01447193	0.0212177	0.03874289
R^2	0.97976983	0.97212801	0.98770182	0.96113565	0.99064607
Higuchi model					
Kh	3.06557435	3.16926353	2.67473544	2.80555293	2.62730873
R^2	0.84394438	0.89391629	0.96134055	0.97622983	0.93466669
Zero Order					
K0	0.20751587	0.21482081	0.18111144	0.19031647	0.17860173
R^2	0.71101283	0.76816738	0.88836367	0.90698189	0.82743861
First Order					
K1	0.47485155	0.49167484	0.41404217	0.43524133	0.40826229
R^2	0.71101283	0.76816738	0.88836367	0.90698189	0.82743861
Hixson–Crowell model					
Khc	0.13168718	0.13649882	0.11489708	0.12079771	0.11393479
R^2	0.72841021	0.78576105	0.95232493	0.91318658	0.84587053

Table 3. Parameters of Korsmeyer–Peppas, Peppas – Sahlin, Higuchi model, Zero Order, First Order, and Hixson–Crowell model of VCC drug release in different drug weights at pH 7.4 and 0.5 M NaCl.

Model / Parameters	2.5mg	5mg	7.5mg	10mg
Korsmeyer–Peppas				
K	45.63244552	34.2797548	25.29977	20.20187
N	0.046912615	0.02072459	0.007966	0.005924452
R^2	0.993357729	0.98192742	0.99255	0.960492486
Peppas - Sahlin				
Kd	0	27.2606959	17.70139897	13.55928499
Kr	45.6324455	7.02332425	7.598558846	6.634990677
M	0.023456307	0.01708044	0.006110065	0.004516449
R^2	0.993357729	0.98208676	0.992633908	0.960696162
Higuchi model				
Kh	4.614900391	3.04467407	2.109294474	1.667667289
R^2	0.929001602	0.93042834	0.953885414	0.984016133
Zero Order				
K0	0.313769265	0.20618662	0.142554008	0.112690168
R^2	0.819238132	0.82214508	0.862546813	0.920456438
First Order				
K1	0.71955313	0.47179029	0.325244395	0.256467972
R^2	0.819238132	0.82214508	0.862546813	0.920456438
Hixson–Crowell model				
Khc	0.2001646	0.13105413	0.090263088	0.071339008
R^2	0.839251957	0.83183222	0.865612099	0.921889779

The Korsmeyer-Peppas model, a semiempirical approach, elucidates the exponential correlation between drug release and time. As the Korsmeyer-Peppas model inspects the release of the drug from a hydrophilic polymer-based system (Rostamitabar et al., 2021), This model ideally depicts the VCC drug release as chitosan serves as a hydrophilic polymer-based system according to literature. The calculated values of the Venivel Chitosan Composite release amount in pH 1, pH 2.5, pH 4, pH 5.5, pH 7, pH 7.4, pH 8.5, pH 10, 0.1M NaCl, 0.2M NaCl, 0.3M NaCl, 0.4M NaCl, 0.5M NaCl, pH 7.4 and 0.5M NaCl in 2.5mg, pH 7.4 and 0.5M NaCl in 5mg, pH 7.4 and 0.5M NaCl in 7.5mg and, pH 7.4 and 0.5M NaCl in 10 mg using the Korsmeyer-Peppas Peppas - Sahlin models align with the experimental cumulative release values, exhibiting a strong correlation coefficient (R^2). A study conducted by (Abdul Hameed et al., 2020) stated, "In the Korsmeyer-Peppas model, the value of n < 0.5, which indicated the dependent of the drug release mechanism on Fickian diffusion or quasi-Fickian diffusion and the transport of the drug occurred via polymer frameworks not via penetration of solvent''. Similarly, in the Peppas-Sahlin model, K1 values were more significant than K2, which implies a release mechanism entirely based on Fickian diffusion. In the present study in the Korsmeyer-Peppas model, as mentioned in Table, the value of n is lower than 0.5 for all samples. Therefore, it is indicated that the Venivel Chitosan Composite drug release mechanism depends on Fickian diffusion. Moreover, the investigation substantiated that the transportation of the VCC drug occurred through polymer frameworks. Among the six models used in this study, the best-

fit model was the Korsmeyer-Peppas Model, which provided the highest R^2 value.

Conclusion

This study highlights the potential of Venivel Chitosan Composite (VCC) in Ayurvedic drug delivery, particularly for wound healing applications. The drug release profile of VCC exhibited a gradual release over 4.5 hours, predominantly through diffusion, making it a promising candidate for further development in targeted and controlled Ayurvedic drug delivery systems.

References

Abdul Hameed, M. M., Mohamed Khan, S. A. P., Thamer, B. M., Al-Enizi, A., Aldalbahi, A., El-Hamshary, H., & El-Newehy, M. H. (2020). Core-shell nanofibers from poly (vinyl alcohol) based biopolymers using emulsion electrospinning as drug delivery system for cephalexin drug. Journal of Macromolecular Science, Part A: Pure and Applied Chemistry, 58(2), 130–144. https://doi.org/10.1080/10601325.2020.1832517

Ali, A., Chiang, Y. W., & Santos, R. M. (2022). X-Ray Diffraction Techniques for Mineral Characterization: A Review for Engineers of the Fundamentals, Applications, and Research Directions. Minerals, 12(2). https://doi.org/10.3390/min12020205

Alworth, L. C., & Harvey, S. B. (2012). Anatomy, Physiology, and Behavior. In The Laboratory Rabbit, Guinea Pig, Hamster, and Other Rodents (pp. 955–966). Elsevier. https://doi.org/10.1016/B978-0-12-380920-9.00039-0

Asadian-Ardakani, V., Saber-Samandari, S., & Saber-Samandari, S. (2016a). The effect of hydroxyapatite in biopolymer-based scaffolds on release of naproxen sodium. Journal of Biomedical Materials Research - Part A, 104(12), 2992–3003. https://doi.org/10.1002/jbm.a.35838

Asadian-Ardakani, V., Saber-Samandari, S., & Saber-Samandari, S. (2016b). The effect of hydroxyapatite in biopolymer-based scaffolds on release of naproxen sodium. Journal of Biomedical Materials Research - Part A, 104(12), 2992–3003. https://doi.org/10.1002/jbm.a.35838

Banerjee, S., Biswas, S., Chanda, A., Das, A., & Adhikari, A. (2014). Evaluation of phytochemical screening and anti inflammatory activity of leaves and stem of Mikania scandens (l.) wild. Annals of Medical and Health Sciences Research, 4(4), 532. https://doi.org/10.4103/2141-9248.139302

Bitrus, A. A., Peter, O. M., Abbas, M. A., & Goni, M. D. (2018). Staphylococcus aureus: A Review of Antimicrobial Resistance Mechanisms. Veterinary Sciences: Research and Reviews, 4(2). https://doi.org/10.17582/journal.vsrr/2018/4.2.43.54

Brand-Williams, W., Cuvelier, M. E., & Berset, C. (1995). Use of a free radical method to evaluate antioxidant activity. LWT - Food Science and Technology, 28(1), 25–30. https://doi.org/10.1016/S0023-6438(95)80008-5

Danapur, V., Haleshi, C., & Sringeswara, A. N. (2020). Endangered medicinal plant coscinium fenestratum (Gaertn.) Colebr. - A Review. In Pharmacognosy Journal (Vol. 12, Issue 5, pp. 1077–1085). EManuscript Technologies. https://doi.org/10.5530/PJ.2020.12.152

Davis, J. L. (2018). Pharmacologic Principles. In Equine Internal Medicine (pp. 79–137). Elsevier. https://doi.org/10.1016/B978-0-323-44329-6.00002-4

Desai, N., Rana, D., Salave, S., Gupta, R., Patel, P., Karunakaran, B., Sharma, A., Giri, J., Benival, D., & Kommineni, N. (2023). Chitosan: A Potential Biopolymer in Drug Delivery and Biomedical Applications. Pharmaceutics, 15(4), 1313. https://doi.org/10.3390/pharmaceutics15041313

Fan, Y., Chen, J., Shirkey, G., John, R., Wu, S. R., Park, H., & Shao, C. (2016). Applications of structural equation modeling (SEM) in ecological studies: an updated review. In Ecological Processes (Vol. 5, Issue 1). Springer Verlag. https://doi.org/10.1186/s13717-016-0063-3

Grigore, M. E., Biscu, E. R., Holban, A. M., Gestal, M. C., & Grumezescu, A. M. (2016). Methods of Synthesis, Properties and Biomedical Applications of CuO Nanoparticles. Pharmaceuticals (Basel, Switzerland), 9(4). https://doi.org/10.3390/ph9040075

Jayanetti, M. (n.d.). Qualitative Phytochemical Screening and Antibacterial Evaluation of Sohphlang-Flemingia vestita. https://www.researchgate.net/publication/362558566

Khatun, A., Rahman, M., Al Nayeem, A., & Rahman, S. (2011). Evaluation of phytochemical and pharmacological properties of Mikania cordata (Asteraceae) leaves. Article in Journal of Pharmacognosy and Phytotherapy, 3(8), 118–123. http://www.academicjournals.org/JPP